

# Frequency beating and damping of breathing oscillations of a harmonically trapped one-dimensional quasicondensate

F. A. Bayocboc, Jr. and K. V. Kheruntsyan

*School of Mathematics and Physics, The University of Queensland, Brisbane, Queensland 4072, Australia*

(Dated: December 1, 2023)

We study the breathing (monopole) oscillations and their damping in a harmonically trapped one-dimensional (1D) Bose gas in the quasicondensate regime using a finite-temperature classical field approach. By characterizing the oscillations via the dynamics of the density profile's rms width over long time, we find that the rms width displays beating of two distinct frequencies. This means that 1D Bose gas oscillates not at a single breathing mode frequency, as found in previous studies, but as a superposition of two distinct breathing modes, one oscillating at frequency close to  $\sim\sqrt{3}\omega$  and the other at  $\sim 2\omega$ , where  $\omega$  is the trap frequency. The breathing mode at  $\sim\sqrt{3}\omega$  dominates the beating at lower temperatures, deep in the quasicondensate regime, and can be attributed to the oscillations of the bulk of the density distribution comprised of particles populating low-lying, highly-occupied states. The breathing mode at  $\sim 2\omega$ , on the other hand, dominates the beating at higher temperatures, close to the nearly ideal Bose gas regime, and is attributed to the oscillations of the tails of the density distribution comprised of thermal particles in higher energy states. The two breathing modes have distinct damping rates, with the damping rate of the bulk component being an order of magnitude larger than that of the tails component, and at least 2–3 times smaller than the damping rate predicted by Landau's theory of damping in 1D.

## I. INTRODUCTION

The study of low-energy excitations and their damping is an indispensable tool for the understanding of collective many-body effects in ultracold quantum gases. In particular, the temperature dependence of the frequency of collective oscillations and their damping have been the subject of scrutiny both experimentally [1–5] and theoretically [6–17] since the first experiments in dilute gas Bose-Einstein condensates [18–20]. Depending on the temperature of the gas, the damping of collective oscillations in harmonically trapped 3D systems has been explained either via collisional relaxation [13, 21], where the two parts of the Bose gas (condensate and thermal components) exchange energy and particles, or via mean-field effects that can lead to Landau or Beliaev mechanisms of damping [6, 7, 11, 16, 22]. The lifetime of collective oscillations in such systems has been predicted and measured to be typically on the order of tens of milliseconds.

In contrast to 3D systems, collective oscillations in one-dimensional (1D) Bose gases damp out on a significantly longer time scales. For example, the lifetime of breathing mode oscillations observed in Ref. [23] in a weakly interacting 1D quasicondensate was on the order of seconds; in the related collisional dynamics of a quantum Newton's cradle in the opposite, strongly interacting regime, the thermalization time constant was estimated to be even longer (longer than  $\sim 70$  seconds) [24]. The slow relaxation rates in the 1D Bose gas are related to the fact that the underlying theoretical model—the Lieb-Liniger model [25, 26]—is integrable in the uniform limit, which puts additional constraints on the pathways to equilibration compared to those present in generic (non-integrable) quantum systems. More specifically, the integrable uniform 1D Bose gas is expected to relax to a generalized Gibbs ensemble rather than to the canon-

ical thermal state [27–33]. In inhomogeneous 1D Bose gases, such as the harmonically trapped 1D quasicondensate studied here, the integrability breaks down and provides a mechanism for relaxation to a thermal ensemble [34]. Nevertheless, for sufficiently weak confinement, the system can be regarded as nearly-integrable and hence is expected to undergo a crossover from transient relaxation to the generalized Gibbs state to a slow decay to the final thermal ensemble [32]. The overall 1D damping rate is expected to be small enough to be neglected in experiments. However, in current experiments the observed relaxation rates in quasi-1D systems are often affected by transverse excitations [35–38] due to the 3D nature of realistic trapping potentials. Such transverse excitations speed up thermalization, thus hampering the characterization of pure 1D damping. Because of this, pure 1D damping rates have not been scrutinized experimentally yet, particularly in the weakly interacting regime of the 1D Bose gas, whereas theoretically the question of 1D thermalization has started to attract attention only relatively recently [39–41].

In this paper, we study damping rates of a finite-temperature weakly interacting 1D Bose gas, following an excitation of breathing mode oscillations in a harmonic trap. The specific scenario that we consider is a sudden trap quench from the initial trap frequency  $\omega_0$  to a slightly smaller frequency  $\omega$ , which invokes breathing oscillations; we simulate these oscillations and their relaxation dynamics using a classical field (*c*-field) approach. In doing so, we also revisit and scrutinize the question of the frequency of breathing oscillations, which has been addressed previously both experimentally [23, 42, 43] and theoretically [44–52].

According to the most recent study by Fang *et al.* [23], the frequency of such oscillations in the root-mean-square (rms) width of the real-space density profile undergoes a

smooth transition from  $\omega_B \simeq \sqrt{3}\omega$  deep in the quasicondensate regime to  $\omega_B \simeq 2\omega$  in the nearly ideal Bose gas regime as the temperature of the gas is increased. In contrast to this, our numerical experiment reveals the presence of both oscillation frequencies in a broad range of temperatures within the quasicondensate regime. We refer to these frequencies as  $\omega_{B1}$  and  $\omega_{B2}$  and attribute the breathing modes at  $\omega_{B1} \simeq \sqrt{3}\omega$  and  $\omega_{B2} \simeq 2\omega$ , respectively, to the oscillations of the bulk and the tail components of the density profile. The observation of two simultaneous breathing modes is made possible by extending our dynamical simulations to significantly longer durations than currently possible experimentally, which reveals an oscillatory pattern (in the rms width) characteristic of beating of two frequencies. Such beating in breathing oscillations, resulting in ‘collapses’ and ‘revivals’ of the rms width of the density profile, is similar to the one recently observed in a partially condensed 3D Bose-Einstein condensate [53].

Finally, we extract the damping rates of these two distinct breathing modes from the  $c$ -field simulations and find that the damping rate  $\Gamma_1$  associated with the breathing mode  $\omega_{B1}$  is on the order of  $\Gamma_1 \simeq 0.08\omega$  (where we use  $1/\omega$  as the timescale), whereas the damping rate  $\Gamma_2$  associated with  $\omega_{B2}$  is an order of magnitude smaller. At the same time, we find that  $\Gamma_1$  is at least 2–3 times smaller than the Landau damping rate predicted in Ref. [54] for a 1D quasicondensate.

## II. $C$ -FIELD METHOD FOR SIMULATING BREATHING OSCILLATIONS

The breathing mode oscillations of a 1D Bose gas in the quasicondensate regime are simulated using the  $c$ -field (or classical field) approach as in Refs. [41, 52, 55]. In this approach [56, 57], the initial thermal equilibrium state of the system is prepared by evolving the simple growth stochastic projected Gross-Pitaevskii equation (SPGPE) for the complex  $c$ -field  $\Psi_{\mathbf{C}}(x, t)$ ,

$$d\Psi_{\mathbf{C}}(x, t) = \mathcal{P}^{(\mathbf{C})} \left\{ -\frac{i}{\hbar} \mathcal{L}_0^{(\mathbf{C})} \Psi_{\mathbf{C}}(x, t) dt + \frac{\Gamma}{k_B T} (\mu - \mathcal{L}_0^{(\mathbf{C})}) \Psi_{\mathbf{C}}(x, t) dt + dW_{\Gamma}(x, t) \right\}, \quad (1)$$

with  $x$  and  $t$  being the position and time, respectively. Here, the projection operator  $\mathcal{P}^{(\mathbf{C})}\{\cdot\}$  sets up the high-energy cutoff [58] between the coherent ( $c$ -field) and the incoherent regions,  $\Gamma$  is the growth rate,  $T$  is the temperature of the effective reservoir (served by the incoherent region) to which the system is coupled, and  $\mu$  is the chemical potential of the reservoir that controls the number of particles in the  $c$ -field region. In addition,  $\mathcal{L}_0^{(\mathbf{C})}$  is the Gross-Pitaevskii operator defined by

$$\mathcal{L}_0^{(\mathbf{C})} = -\frac{\hbar^2}{2m} \frac{\partial^2}{\partial x^2} + V(x) + g|\Psi_{\mathbf{C}}(x, t)|^2, \quad (2)$$

where  $V(x)$  is the external trapping potential, which we assume is harmonic,  $V(x) = \frac{1}{2}m\omega_0^2 x^2$ , with frequency  $\omega_0$ , and  $g$  is the strength of repulsive ( $g > 0$ ) interatomic contact interaction in 1D. The last term,  $dW_{\Gamma}(x, t)$ , in Eq. (1) is a complex-valued stochastic white noise satisfying the following nonzero correlation:

$$\langle dW_{\Gamma}^*(x, t) dW_{\Gamma}(x', t) \rangle = 2\Gamma \delta(x - x') dt. \quad (3)$$

Evolving the above SPGPE from an arbitrary initial state and for sufficiently long time (such that the memory of the initial state is lost) samples finite-temperature equilibrium configurations of the system from the grand-canonical ensemble. Averages over a large number of stochastic realizations of the  $c$ -field  $\Psi_{\mathbf{C}}(x, t)$  and its complex conjugate  $\Psi_{\mathbf{C}}^*(x, t)$  are then used to construct thermal equilibrium values of physical observables that can be expressed in terms of expectation values of standard bosonic quantum field operators  $\hat{\Psi}(x, t)$  and  $\hat{\Psi}^\dagger(x, t)$ , except that their quantum commuting nature is ignored. As an example, the particle number density  $\rho(x, t) = \langle \hat{\Psi}^\dagger(x, t) \hat{\Psi}(x, t) \rangle$  in the  $c$ -field approach is calculated as the stochastic average  $\rho(x, t) = \langle \Psi_{\mathbf{C}}^*(x, t) \Psi_{\mathbf{C}}(x, t) \rangle$  (where the brackets  $\langle \dots \rangle$  now refer to stochastic averaging over a large number of stochastic trajectories), whereas the momentum distribution  $n(k, t)$ , where  $k$  is in wave-number units, is calculated as  $n_j(k, t) = \iint dx dx' e^{ik(x-x')} \langle \Psi_{\mathbf{C}}^*(x, t) \Psi_{\mathbf{C}}(x', t) \rangle$ .

The thermal equilibrium configurations (stochastic realizations) of the  $c$ -field  $\Psi_{\mathbf{C}}(x, t)$  prepared via the SPGPE are regarded as forming the initial ( $t = 0$ ) thermal equilibrium state of the system. The  $c$ -field realizations can then be evolved according to the standard mean-field Gross-Pitaevskii equation,

$$i\hbar \frac{\partial}{\partial t} \Psi_{\mathbf{C}}(x, t) = \mathcal{L}_0^{(\mathbf{C})} \Psi_{\mathbf{C}}(x, t), \quad (4)$$

which simulates the subsequent real-time dynamics of a closed system in response to a particular dynamical protocol, such as a confinement or interaction quench.

The dynamical protocol that we use here to invoke the breathing mode oscillations is a sudden quench (at time  $t = 0$ ) of the harmonic trap frequency from  $\omega_0$  to a new value  $\omega$ . The strength of such a quench can be characterized by

$$\epsilon = \left( \frac{\omega_0}{\omega} \right)^2 - 1, \quad (5)$$

which can be either smaller or larger than zero depending on the ratio  $\omega_0/\omega$ . For  $|\epsilon| \ll 1$ , the numerical value of  $\epsilon$  can be used to determine the amplitude of breathing mode oscillations [52].

Breathing oscillations of a 1D quasicondensate in this particular scenario have been studied previously experimentally and theoretically in Refs. [23, 52]. The focus of those works was the understanding of the phenomenon of frequency doubling of the oscillations in momentum space. In the present work, we instead concentrate on

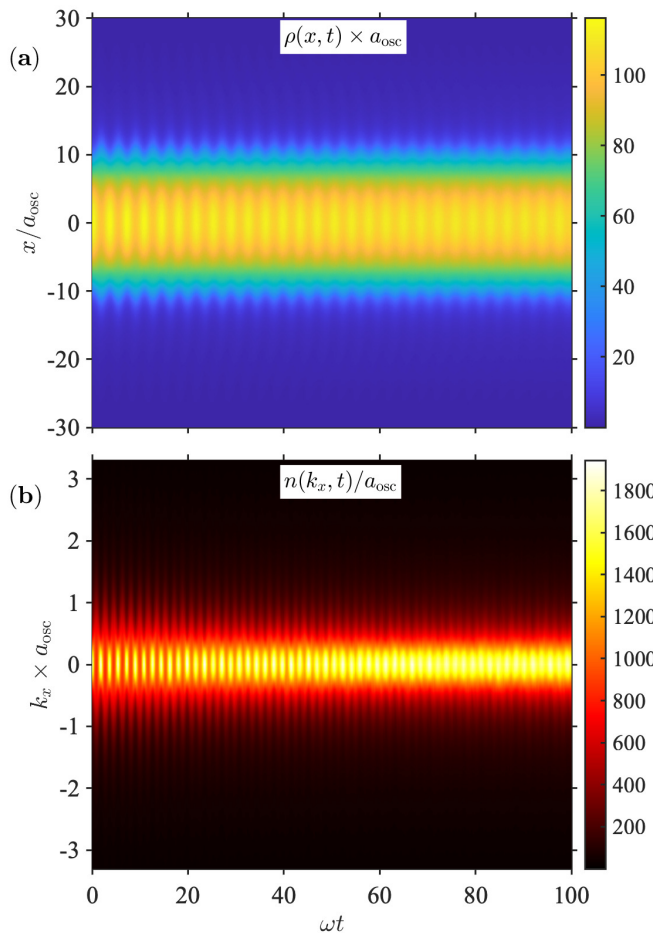


FIG. 1. Typical evolution of the real-space density profile  $\rho(x,t)$  and the momentum distribution  $n(k_x,t)$  of a quasicondensate after a quench of the longitudinal trapping potential  $\omega_0 \rightarrow \omega$ , with a quench strength  $\epsilon \simeq 0.235$  ( $\omega/\omega_0 = 0.9$ ). The initial condition of the system is characterized by  $\gamma_0^{3/2}\bar{\tau} = 0.1$ . The dimensionless position ( $x/a_{osc}$ ) and momentum ( $ka_{osc}$ ) are introduced with respect to the initial harmonic oscillator length  $a_{osc} = \sqrt{\hbar/m\omega_0}$  serving as the lengthscale, whereas the time is normalized to  $1/\omega$ .

analysing the damping of the breathing mode oscillations seen in Refs. [23, 52], in analogy with a recent work on thermalization of a 1D quasicondensate in a quantum Newton's cradle setup [41].

In Fig. 1, we show typical evolution of the density profile  $\rho(x,t)$  and the respective momentum distribution  $n(k_x,t)$ , after a quench of the trap frequency as described above. In this example, the initial state is characterized by  $\gamma_0^{3/2}\bar{\tau} = 0.1$ , and the quench strength is  $\epsilon = 0.235$ . Here,  $\gamma_0 = mg/\hbar^2\rho(0)$  is the dimensionless interaction strength evaluated at the initial peak density  $\rho_0$  and  $\bar{\tau} = 2\hbar^2k_B T/mg^2$  is the dimensionless temperature of the system (for further details on the parameter regimes of a 1D quasicondensate, see Sec. III A below). We see here that both  $\rho(x,t)$  and  $n(k_x,t)$  breathe af-

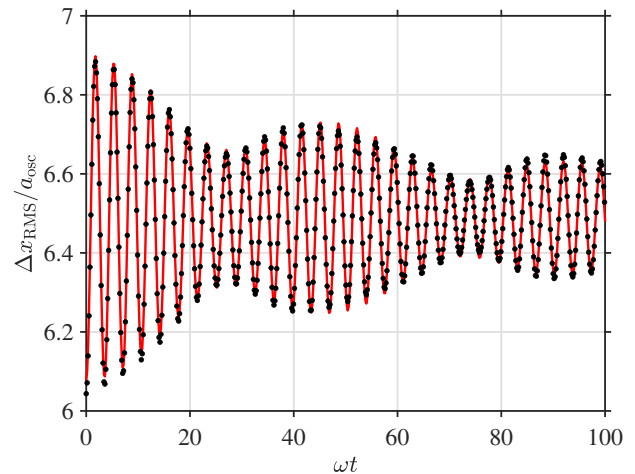


FIG. 2. Root-mean-square width  $\Delta x_{RMS}(t)$  of the density profile  $\rho(x,t)$  shown in Fig. 1(a), normalized to harmonic oscillator length  $a_{osc} = \sqrt{\hbar/m\omega_0}$ . The black dots are data points from  $c$ -field simulations, whereas the red line is a fit using Eq. (7).

ter the quench, with  $n(k_x,t)$  breathing with twice the frequency of breathing of  $\rho(x,t)$ . This phenomenon is known as frequency doubling [23] and can be interpreted, via a classical hydrodynamic approach [52] as a result of a self-reflection mechanism due to the mean-field interaction energy barrier. Similarly to the results of Ref. [52], we observe the frequency doubling in this finite temperature example because the system under these parameters is in the quasicondensate regime where the contribution of the hydrodynamic velocity field dominates the contribution of the thermal velocities (which show no frequency doubling) of the breathing dynamics of the momentum distribution. As the system evolves in time the oscillations in both the density and momentum distributions can be seen to damp out, with the damping somewhat more apparent in the momentum distribution.

### III. BREATHING DYNAMICS

To further characterize the dynamics and damping of the breathing oscillations, we calculate the rms width of the density profile given by

$$\Delta x_{RMS}(t) = \frac{1}{\sqrt{N}} \left[ \int dx \rho(x,t) x^2 - \left( \int dx \rho(x,t) x \right)^2 \right]^{1/2}, \quad (6)$$

where  $N = \int dx \rho(x)$  is the total number of particles.

In Fig. 2, we show the calculated  $\Delta x_{RMS}(t)$  as a function of time, for the density profile  $\rho(x,t)$  of Fig. 1(a). A distinct feature of the rms width oscillations is the presence of beating, which is not apparent in Fig. 1(a). This beating suggests that the quasicondensate, after the quench of the trapping potential, oscillates not at a single

breathing mode frequency, but as a superposition of two distinct frequencies.

To extract the beating frequencies from the oscillations of the rms width, we fit a sum of two cosine function with two distinct frequencies, and each with its own damping term,

$$\Delta x_{\text{RMS}}(t) = A_1 \cos(\omega_{B1}t + \phi_1)e^{-\Gamma_1 t} + A_2 \cos(\omega_{B2}t + \phi_2)e^{-\Gamma_2 t} + C. \quad (7)$$

Here,  $\omega_{Bi}$  ( $i = 1, 2$ ) are the two breathing mode frequencies,  $A_i$ ,  $\Gamma_i$  and  $\phi_i$  are the respective amplitudes, damping rates, and the phases of each breathing mode, and the last term  $C$  serves as a constant background. As can be seen from Fig. 2, Eq. (7) fits very well to the rms width  $\Delta x_{\text{RMS}}(t)$  calculated from the  $c$ -field simulations, confirming that the nontrivial oscillatory dynamics of the rms width  $\Delta x_{\text{RMS}}(t)$  is indeed a result of beating of two components of the 1D Bose gas, breathing at two distinct frequencies  $\omega_{B1}$  and  $\omega_{B2}$ .

Similar beating of the rms width has been observed in 3D systems [53], where the effect was referred to as ‘collapses’ and ‘revivals’ of the rms width due to in-phase and out-of-phase oscillations of the condensed and non-condensed fractions of the gas.

### A. Beating frequencies

To understand the emergence of two distinct frequencies in the breathing oscillations of a 1D quasicondensate, we recall the results of Ref. [52], in which the breathing dynamics were studied within the classical hydrodynamic approach. We consider the limiting cases of a classical ideal (noninteracting) gas and a weakly interacting 1D Bose gas deep in the quasicondensate regime. The regimes of a harmonically trapped 1D Bose gas can be characterized [59] by two dimensionless parameters: the dimensionless interaction strength in the trap centre,  $\gamma_0 = mg/\hbar^2 \rho_0$  (where  $\rho_0 \equiv \rho(0)$  is the peak density), and the dimensionless global temperature,  $\bar{\tau} = 2\hbar^2 k_B T / mg^2$ . In terms of these parameters, the classical ideal gas regime corresponds to  $\bar{\tau} \gg 1$  and  $\gamma_0^{3/2} \bar{\tau} \gg 1$ , whereas the quasicondensate regime, dominated by thermal fluctuations (rather than zero-point vacuum fluctuations), corresponds to  $\sqrt{\gamma_0} \ll \gamma_0^{3/2} \bar{\tau} \ll 1$  (hence  $\gamma_0 \ll 1$ ). The frequencies of breathing mode oscillations in these two regimes, found from hydrodynamic scaling solutions [52], are given by  $\omega_B = 2\omega$  in the ideal gas regime and by  $\omega_B = \sqrt{3}\omega$  in the quasicondensate regime.

Other theoretical and experimental studies of harmonically trapped 1D Bose gas [23, 42, 43, 45, 47–51], have predicted and observed these breathing mode oscillation frequencies. Furthermore, for a zero temperature gas, the breathing mode dynamics was predicted [49] to display the so-called reentrant behaviour, wherein the frequency of oscillations was shown to undergo a smooth crossover from the ideal Bose gas value of  $2\omega$  down to  $\sqrt{3}\omega$  in

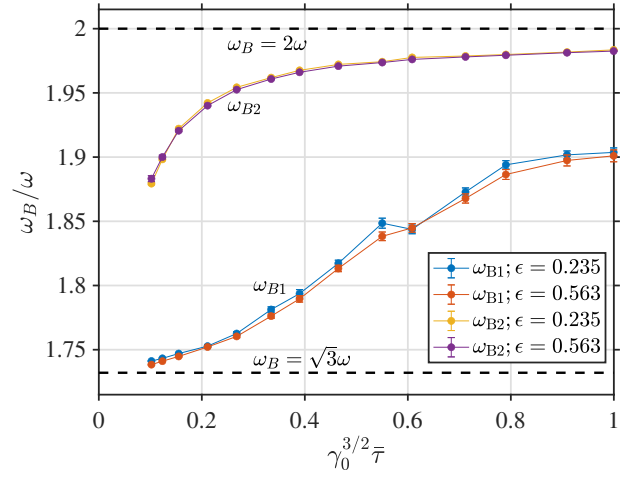


FIG. 3. Breathing mode frequencies  $\omega_{B1}$  and  $\omega_{B2}$  as a function of  $\gamma_0^{3/2}\bar{\tau}$  extracted from  $c$ -field simulations by using the fitting equation Eq. (7). The error bars account for fitting error only and indicate a 95% confidence interval. Two different sets of data points correspond to two values of the trap quench strength  $\epsilon$  used in the simulations,  $\epsilon \simeq 0.235$  ( $\omega/\omega_0 = 0.9$ ) and  $\epsilon \simeq 0.563$  ( $\omega/\omega_0 = 0.8$ ).

the weakly interacting gas, and then back to  $2\omega$  in the strongly interacting regime.

However, as we have seen from finite-temperature  $c$ -field simulations of the previous section, the breathing oscillations in a finite temperature quasicondensate display a beating of two distinct frequencies. This suggests that in a weakly interacting 1D Bose gas, the bulk of the quasicondensate density near the trap centre, where the interactions are more important, oscillates at the frequency close to  $\sqrt{3}\omega$ , whereas the tails of the density distribution, behaving more like a classical ideal gas, oscillate at the frequency  $2\omega$ . To confirm this hypothesis, we now simulate the dynamics of breathing oscillations for a range of different values of the dimensionless parameter  $\gamma_0^{3/2}\bar{\tau}$ , varying it the range  $0.07 < \gamma_0^{3/2}\bar{\tau} < 1$ , and hence scanning our system from deep quasicondensate regime towards the crossover boundary with the nearly classical ideal gas (beyond which the  $c$ -field method is no longer applicable). Upon doing so, we extract the breathing mode frequencies  $\omega_{Bi}$  ( $i=1, 2$ ) and the respective damping rates  $\Gamma_i$  by fitting the rms width of the density distribution to Eq. (7) for each value of  $\gamma_0^{3/2}\bar{\tau}$ .

In Fig. 3, we show the extracted frequencies as a function of  $\gamma_0^{3/2}\bar{\tau}$ , for two different values of the quench strength  $\epsilon$ . As we see, in both cases and for smaller values of  $\gamma_0^{3/2}\bar{\tau}$ , the extracted breathing mode frequencies are approximately equal to  $\omega_{B1} \approx \sqrt{3}\omega$  and  $\omega_{B2} \approx 2\omega$ . As the dimensionless parameter  $\gamma_0^{3/2}\bar{\tau}$  is increased towards the classical ideal gas regime  $\gamma_0^{3/2}\bar{\tau} \simeq 1$ , the frequencies of both components increase too, with  $\omega_{B1}$  deviating further away from the value of  $\sqrt{3}\omega$  and both  $\omega_{B1}$  and  $\omega_{B2}$



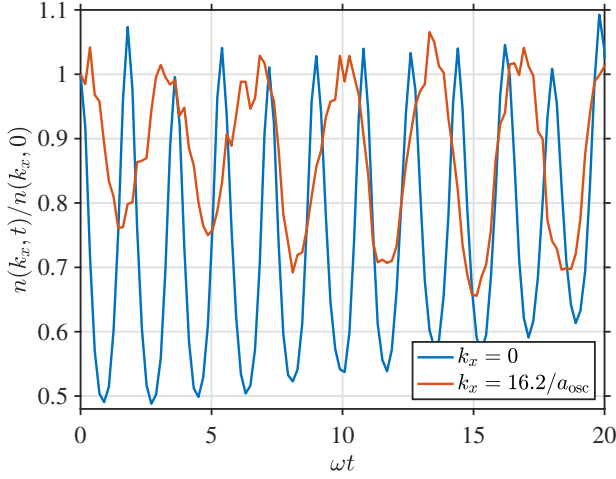


FIG. 4. Evolution of the momentum distribution  $n(k_x, t)$  at  $k_x = 0$  and at  $k_x = 16.2/a_{\text{osc}}$ , for  $\gamma_0^{3/2}\bar{\tau} = 0.1$  and  $\epsilon = 0.235$ . The momentum distribution at  $k_x = 0$  displays frequency doubling and oscillates at  $\omega^{(k)} \simeq 2\omega_{B1}$ , which is characteristic of a system deep in the quasicondensate regime. On the other hand, the momentum distribution at  $k_x = 16.2/a_{\text{osc}}$  does not display frequency doubling (and oscillates at  $\omega^{(k)} \simeq \omega_{B2}$ ), which is characteristic of a classical ideal gas regime.

approaching closer to  $2\omega$ .

We can therefore identify the frequencies  $\omega_{B1}$  and  $\omega_{B2}$ , respectively, with the breathing mode oscillations of the bulk of the quasicondensate near the trap centre (dominated by high-occupancy, low-energy states) and the tails of the density profile (dominated by low-occupancy, high-energy states). Indeed, particles near the trap centre have the local value of  $\gamma_x^{3/2}\bar{\tau} < 1$  (with  $\gamma_x = mg/\hbar^2\rho(x)$ ) and hence are deeper in the quasicondensate regime, whereas particles in the tails of the density distribution have the local value of  $\gamma_x^{3/2}\bar{\tau} \gtrsim 1$  and can be approximated as noninteracting, ideal gas particles.

This conclusion can be further verified if we inspect the dynamics of the momentum distribution of the 1D Bose gas,  $n(k_x, t)$ . In Fig. 4, we can see the difference in behaviour of the momentum distribution  $n(k_x, t)$  at  $k_x = 0$  and at  $k_x = 16.2/a_{\text{osc}}$ . While the oscillations of the momentum distribution at  $k_x = 0$  display frequency doubling ( $\omega^{(k)} = 2\omega_{B1}$ ), a property of a Bose gas deep in the quasicondensate regime, the momentum distribution at  $k_x = 16.2/a_{\text{osc}}$  does not ( $\omega^{(k)} = \omega_{B2}$ ). In addition, a simple sinusoidal fit to both curves in Fig. 4 yields breathing frequency of  $\omega_{B1} \approx 1.74\omega$  for  $n(k_x = 0, t)$  and  $\omega_{B2} \approx 1.87\omega$  for  $n(k_x = 16.2/a_{\text{osc}}, t)$ . These frequencies are close to the breathing mode frequencies we have in Fig. 3 extracted from the rms width of the respective density distribution for  $\gamma_0^{3/2}\bar{\tau} = 0.1$ . Thus, from this point onwards, we will refer to the component with breathing frequency  $\omega_{B1}$  as the *bulk* component, whereas the component with breathing frequency  $\omega_{B2}$  will be referred to as the *tail* component.

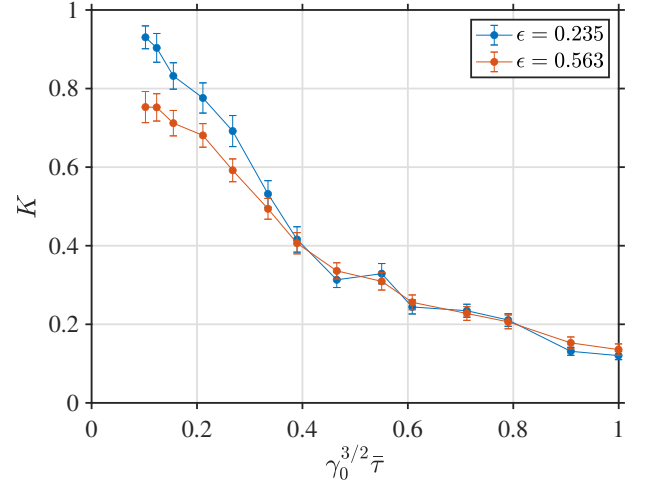


FIG. 5. Relative power  $K$  of the bulk component in the breathing oscillations of a 1D quasicondensate as a function of  $\gamma_0^{3/2}\bar{\tau}$  for two different quench strengths  $\epsilon$ . The error bars account for the fitting error only and indicate a 95% confidence interval.

We pause here momentarily to emphasize the key difference between our findings and the previous studies of breathing mode oscillations in a weakly interacting 1D Bose gas. While previous studies have also predicted a smooth crossover of the oscillation frequency from  $\sim\sqrt{3}\omega$  to  $\sim 2\omega$  as the temperature is increased, the frequency in question has always been what we refer here to as the oscillations of the bulk component  $\omega_{B1}$ . While we observe the same crossover for the  $\omega_{B1}$  component, our simulations indicate that: (i) there is a second distinct breathing frequency  $\omega_{B2}$ , which is for the tail component, and (ii)  $\omega_{B2}$  undergoes a similar crossover from  $\sim\sqrt{3}\omega$  to  $\sim 2\omega$  while remaining different to  $\omega_{B1}$ . In the limiting cases of  $\gamma_0^{3/2}\bar{\tau} \sim 1$  (nearly classical ideal gas) and  $\gamma_0^{3/2}\bar{\tau} \ll 1$  (deep in quasicondensate regime) the two frequencies become nearly degenerate, both tending towards either  $2\omega$  or  $\sqrt{3}\omega$  in the respective limits. The change from one breathing frequency to two frequencies and then back to one can be explained by considering how particles occupy different energy modes at different values of  $\gamma_0^{3/2}\bar{\tau}$ . For system parameters deep in the quasicondensate regime ( $\gamma_0^{3/2}\bar{\tau} \ll 1$ ), all particles occupy the low-energy states, and the whole system exhibits collective breathing oscillations ( $\omega_{B1}$ ) close to the pure mean-field behaviour of a zero-temperature system. As we go to higher values of  $\gamma_0^{3/2}\bar{\tau}$  (by, e.g., increasing the temperature of the system, or reducing the peak density  $\rho_0$  and hence increasing  $\gamma_0$ ), a larger fraction of particles begin to thermally populate higher energy states, and a second breathing mode ( $\omega_{B2}$ ) with behaviour closer to that of a classical ideal gas emerges. Then, as we reach the nearly ideal gas regime ( $\gamma_0^{3/2}\bar{\tau} \gtrsim 1$ ), almost all of the particles occupy high-energy modes. The collective breath-

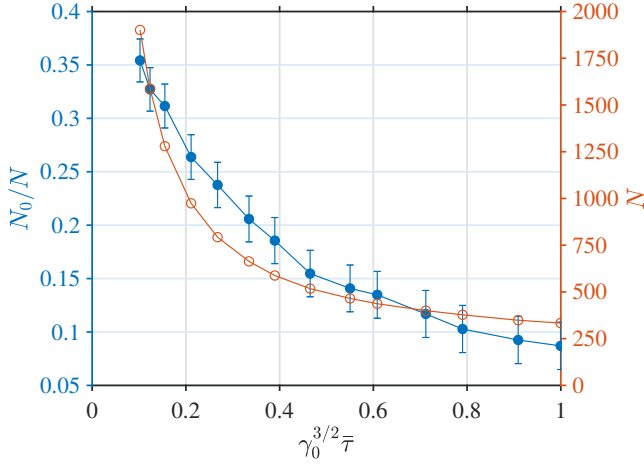


FIG. 6. Computed condensate fraction  $N_0/N$  (full circles, left vertical axis) and the respective total  $N$  (open circles, right vertical axis) of the initial state of the 1D Bose gas as a function of  $\gamma_0^{3/2}\bar{\tau}$ . The different values of  $\gamma_0^{3/2}\bar{\tau}$  were achieved by scanning the chemical potential of the system, which in turn governs the total  $N$  (and hence the peak density  $\rho_0$  and  $\gamma_0$ ), while the temperature and the trap frequency were kept the same.

ing mode, characteristic of low-energy particles, begin to disappear and the whole system starts to again exhibit breathing oscillations with a single frequency  $\omega_{B2}$ .

### B. Relative power of breathing components

To quantify the relative contribution of the beating components (bulk and tail components) to the total breathing oscillations in the intermediate regime,  $0.07 < \gamma_0^{3/2}\bar{\tau} < 1$ , we introduce the relative power of the bulk component,

$$K = \frac{A_1^2}{A_1^2 + A_2^2}. \quad (8)$$

The relative contribution of the tail component is then given by  $1 - K$ , and Eq. (7) for the rms width can be rewritten as

$$\Delta x_{\text{RMS}}(t) = A[\sqrt{K} \cos(\omega_{B1}t + \phi_1)e^{-\Gamma_1 t} + \sqrt{1-K} \cos(\omega_{B2}t + \phi_2)e^{-\Gamma_2 t}] + C, \quad (9)$$

where  $A = \sqrt{A_1^2 + A_2^2}$ .

In Fig. 5, we plot the relative power  $K$  as a function of  $\gamma_0^{3/2}\bar{\tau}$ , for two different values of the quench strengths  $\epsilon$  as in Fig. 3. As we see, the contribution of the bulk component to the breathing mode oscillation decreases with  $\gamma_0^{3/2}\bar{\tau}$ . As we discussed above, this is because the fraction of particles in the tail component, behaving as nearly classical ideal gas, increases with  $\gamma_0^{3/2}\bar{\tau}$ , whereas the fraction of particles in the bulk component decreases.

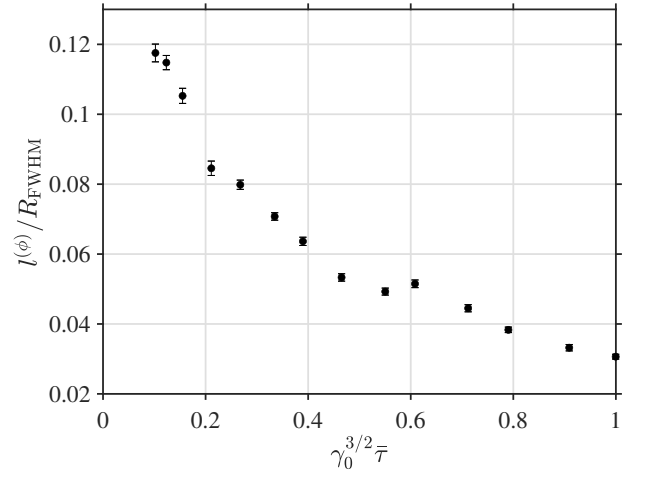


FIG. 7. Computed thermal coherence length of the initial state of the 1D Bose gas at different values of  $\gamma_0^{3/2}\bar{\tau}$ . The error bars account for the fitting error only and indicate a 95% confidence interval.

We note here that the quantitative details of the curves in Fig. 5, such as the value of  $\gamma_0^{3/2}\bar{\tau}$  at which the relative powers of the bulk and tail components are equal to each other ( $K = 0.5$ ), have weak dependence on the high-energy energy cutoff  $\epsilon_{\text{cut}}$  chosen in the SPGPE simulations [58]. Indeed, the cutoff energy  $\epsilon_{\text{cut}}$  dictates how many high-energy particles we include in our system: choosing a higher energy cutoff will increase (decrease) the contribution of the tail (bulk) component, thus shifting the value of  $\gamma_0^{3/2}\bar{\tau}$  at which the curves intersect with  $K = 0.5$  to a slightly lower value than the one that can be extracted from the examples of Fig. 5. The opposite is true if we choose a lower energy cutoff. Despite this weak dependence on  $\epsilon_{\text{cut}}$ , the qualitative behaviour of the curves in Fig. 5 remains the same irrespective of the choice  $\epsilon_{\text{cut}}$ .

A further insight into the composition of the bulk and tail components of the 1D Bose gas can be gained by computing the condensate fraction  $N_0/N$  of the initial state of the system as per Penrose–Onsager criterion [60]. The condensate fraction  $N_0/N$  is plotted in Fig. 6 as a function of  $\gamma_0^{3/2}\bar{\tau}$ , together with the respective total number of atoms in the system  $N$ , where we note that the dimensionless parameter  $\gamma_0^{3/2}\bar{\tau}$  was scanned by changing the total number of particles  $N$  (hence changing the peak density  $\rho_0$  and  $\gamma_0$ ) while maintaining the same absolute temperature  $T$  (and hence the same value of  $\bar{\tau}$ ). As we see, the maximum condensate fraction, that is attained here, is approximately 0.35 at the lowest value of  $\gamma_0^{3/2}\bar{\tau}$ , whereas the minimum condensate fraction is  $\sim 0.09$  at the maximum  $\gamma_0^{3/2}\bar{\tau}$ . For the maximum condensate fraction of only 0.35, the corresponding relative power  $K$  in the oscillations of the bulk component is nearly unity ( $K \sim 0.93$ ). This implies that the bulk component is composed

not only of the particles in the condensate mode, but also of particles in highly-occupied, low-energy states above the condensate mode.

The same conclusion can be arrived at by analyzing an alternative quantity—the initial thermal phase coherence length  $l_\phi$  in the trap centre—which, unlike the condensate fraction, is an intensive quantity. For a uniform quasicondensate at density  $\rho$  and temperature  $T$ , this is given by  $l_\phi = 2\hbar^2\rho/mk_BT$  [61–63]. For a harmonically trapped system, we compute the initial ( $t = 0$ ) thermal phase coherence length in the trap centre by fitting the initial normalized first-order correlation function  $g^{(1)}(x, x'; t=0) = \langle \Psi_C^*(x, 0)\Psi_C(x', 0) \rangle / \sqrt{\rho(x, 0)\rho(x', 0)}$  at  $x' = 0$  with an exponential fit  $g^{(1)}(x, x'; t=0) = \exp(-|x - x'|/2l_\phi)$  [61–64]. Here, the local phase coherence length is expected to be equal to  $l_\phi = 2\hbar^2\rho_0/mk_BT$  (where  $\rho_0 \equiv \rho(0, 0)$  is the initial peak density), in the local density approximation, and our fitted values are indeed very close to this analytic result. The fitted values of  $l_\phi$  as a function  $\gamma_0^{3/2}\bar{\tau}$  are plotted in Fig. 7, where we see qualitatively the same trend as for the condensate fraction  $N_0/N$ . For the lowest value of  $\gamma_0^{3/2}\bar{\tau}$  sampled in Fig. 7, the thermal phase coherence length is only a relatively small fraction ( $\sim 0.12$ ) of the full-width-at-half-maximum (FWHM) of the initial density distribution, yet the relative power  $K$  in the oscillations of the bulk component is nearly unity at the same  $\gamma_0^{3/2}\bar{\tau}$ . This again implies that the bulk component is composed not only of the particles in the locally phase coherent region, physically similar to the condensate fraction, but extends beyond this region.

#### IV. DAMPING OF BREATHING OSCILLATIONS

Having identified that the breathing oscillations of a 1D quasicondensate involve beating of two distinct frequencies, corresponding to the oscillations of the bulk and tail components, we now characterize the respective damping rates,  $\Gamma_1$  and  $\Gamma_2$ , observed in Fig. 2 and extracted from fitting the results of  $c$ -field simulations to Eq. (9). The damping rates extracted in this way are shown in Fig. 8 as a function of  $\gamma_0^{3/2}\bar{\tau}$ , for two different quench strengths  $\epsilon$ . Similarly to the frequencies  $\omega_{B1}$  and  $\omega_{B2}$ , the damping rates  $\Gamma_1$  and  $\Gamma_2$  are different from each other and are independent of the quench strength.

The damping rate  $\Gamma_2$  associated with the frequency  $\omega_{B2}$  of the tail component is significantly smaller than the damping rate  $\Gamma_1$  associated with the frequency  $\omega_{B1}$  of the bulk component. This is consistent with our earlier observation that the particles comprising the tail component behave as a nearly classical ideal gas, which is expected to have very little to no damping. The damping rate  $\Gamma_1$ , on the other hand, is large and increases initially with  $\gamma_0^{3/2}\bar{\tau}$ , before saturating to a value of  $\Gamma_1 \sim 0.08\omega$  at  $\gamma_0^{3/2}\bar{\tau} \sim 0.6$  and then decreasing slightly as we approach the upper boundary of the quasiconden-

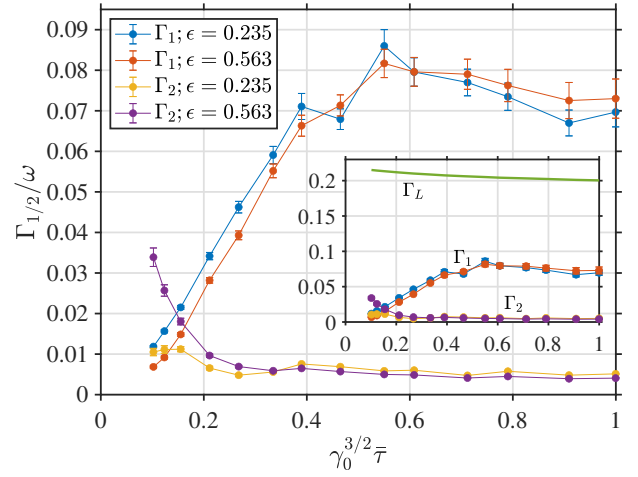


FIG. 8. Damping rates  $\Gamma_i$  ( $i = 1, 2$ ) of the breathing oscillations in a 1D quasicondensate as a function of the dimensionless parameter  $\gamma_0^{3/2}\bar{\tau}$ , for two different quench strengths  $\epsilon$ . The error bars on data points account for the fitting error only, which indicates a 95% confidence interval. In the inset, in addition to the same data, we show the damping rate  $\Gamma_L$  (solid line) calculated from the theory of Landau damping in 1D (see text).

sate regime,  $\gamma_0^{3/2}\bar{\tau} \sim 1$ . For experimentally typical values of  $\omega_0/2\pi \sim 10$  Hz, the damping rate of  $\Gamma_1 \sim 0.08\omega$  corresponds to  $\Gamma_1 \sim 4$  s $^{-1}$  (or a damping time constant of  $\tau_1 = 1/\Gamma_1 \sim 0.25$  s), whereas the damping rate of  $\Gamma_2 \sim 0.008\omega$  ( $\tau_2 = 1/\Gamma_2 \sim 2.5$  s) is an order of magnitude smaller.

Similarly to damping of low-energy collective excitations in a harmonically trapped and partially Bose-condensed 3D systems at finite temperatures, the dominant damping mechanism of the bulk component in our trapped 1D quasicondensate is expected to be Landau damping. In Landau damping, a low-energy collective excitation of energy  $\hbar\omega_{B1}$  and a thermal excitation of energy  $E_i$  are annihilated (created) and another thermal excitation of energy  $E_j$  is created (annihilated). Within the  $c$ -field approach employed in our numerical simulations, this damping mechanism is implicitly present through the interaction term in the GPE for the  $c$ -field  $\Psi_C(x, t)$  as the ‘classical region’ incorporates not only the condensate mode but also many low-lying excited modes that have a relatively high thermal occupation.

Qualitatively, the lowest damping rate of the bulk component,  $\Gamma_1$ , at smallest values  $\gamma_0^{3/2}\bar{\tau}$  that we see in Fig. 8 can be understood because the fraction of particles in the condensate mode is the largest in this regime (see also Fig. 6). Reciprocally, this means that the fraction of particles in the thermal component is the lowest. Accordingly, the processes of interconversion from and into the thermal component contributing to Landau mechanism are inefficient and lead to a low damping rate. The damping rate grows with  $\gamma_0^{3/2}\bar{\tau}$  because such an increase

leads to a larger fraction of particles in the thermal component, which absorb the energy from the condensate component at a faster rate. The subsequent downwards trend of  $\Gamma_1$  at the largest values of  $\gamma_0^{3/2}\bar{\tau}$  is not well understood, and might be an artefact of the  $c$ -field approximation, wherein only a fraction of thermal particles is included in the  $\Psi_C(x, t)$ -field or the ‘classical region’.

An analytic treatment of Landau damping rate  $\Gamma_L$  in a trapped 1D Bose gas can be developed following the approaches of Refs. [6, 7, 11, 16] for 3D systems and adopting the Bogoliubov theory of elementary excitations for 1D quasicondensates [61, 65]. Such a treatment was developed in Ref. [54] for a homogeneous 1D Bose gas, but comes with a caveat (compared to the treatment in 3D) that the common procedure of replacing the delta-function term (in the expression for  $\Gamma_L$ ) by a Lorentzian of finite width  $\Delta$  is not justified in 1D [54]. This is because the calculated damping rate  $\Gamma_L$  does not display any region of  $\Delta$  in which  $\Gamma_L$  changes slowly with  $\Delta$ , as is the case in 3D. As a result, the damping rate cannot be unambiguously determined in 1D by extrapolating back to the value at  $\Delta = 0$ . Instead, the authors of Ref. [54] propose an alternative approach, in which the Landau damping rate is evaluated using the equation

$$\Gamma_L = \frac{1}{\hbar^2} \sum_{ij} |A_{ij}|^2 (f_i - f_j) \frac{3\Gamma_L}{(\omega_{ij} - \omega_{\text{osc}})^2 + (3\Gamma_L)^2}, \quad (10)$$

which can be solved for  $\Gamma_L$  graphically. In this expression,  $f_i \equiv f(E_i) = [e^{E_i/k_B T} - 1]^{-1}$  are standard Bose occupation factors for thermal excitations of energy  $E_i$  at temperature  $T$ , whereas  $A_{ij}$  are the elements

$$\begin{aligned} A_{ij} = & 2g \int dx \Psi_0(x) \\ & \times \{ [u_i(x)u_j^*(x) - v_i(x)u_j^*(x) + v_i(x)v_j^*(x)] u_{\text{osc}}(x) \\ & - [u_i(x)u_j^*(x) - u_i(x)v_j^*(x) + v_i(x)v_j^*(x)] v_{\text{osc}}(x) \} \end{aligned} \quad (11)$$

of the transition matrix that couples the collective mode with the thermal excitations,  $\Psi_0(\mathbf{r})$  being the condensate complex amplitude. The amplitudes of excitation modes,  $u_i(x)$  and  $v_i(x)$ , are obtained by solving the Bogoliubov equations

$$\begin{aligned} \left( -\frac{\hbar^2}{2m} \frac{d^2}{dx^2} + V(x) + 2g|\Psi_0(x)|^2 - \mu \right) u_i(x) \\ - g\Psi_0^2(x)v_i(x) = E_i u_i(x), \end{aligned} \quad (12)$$

$$\begin{aligned} \left( -\frac{\hbar^2}{2m} \frac{d^2}{dx^2} + V(x) + 2g|\Psi_0(x)|^2 - \mu \right) v_i(x) \\ - g[\Psi_0^*(x)]^2 u_i(x) = -E_i v_i(x), \end{aligned} \quad (13)$$

with the condensate collective excitation of interest (the breathing mode, in our case),  $u_{\text{osc}}(x)$  and  $v_{\text{osc}}(x)$ , being already separated out, while satisfying the same Bogoliubov equations. In addition,  $\mu$  is the chemical potential

and  $V(x) = \frac{1}{2}m\omega^2 x^2$  is the trapping potential in which the collective oscillations are taking place.

By solving the above Bogoliubov equations numerically, we then calculate the transition matrix elements  $A_{ij}$ , and find the Landau damping rate  $\Gamma_L$  from Eq. (10) (hence extending the results of Ref. [54] for a homogeneous system to the harmonically trapped case). The damping rate  $\Gamma_L$  found in this way is shown in the inset of Fig. 8 as a solid line. For a broad range of values of  $\gamma_0^{3/2}\bar{\tau}$ , the Landau damping rate is at least 3–4 times larger than the damping rate  $\Gamma_1$  found from our numerical simulations. The reason for this discrepancy deserves a further study, but can be qualitatively explained by the classical field approximation, wherein the  $\Psi_C(x, t)$  field or the ‘classical region’ includes only a fraction of thermal particles, hence underestimating the damping rate  $\Gamma_1$ . At the same time, the theory of Landau damping conventionally assumes that the thermal excitations are always in thermal equilibrium, whereas this assumption does not apply to our system because quenching the trapping frequency also excited a collective breathing oscillation of the tail component, which acts as a dynamical (rather than a static) bath of thermal excitations. In an equivalent quench scenario in a 3D system, these questions can, in principle, be addressed using, e.g., the Zaremba–Nikuni–Griffin (ZNG) formalism [21, 66], where the condensate part of the system is described by the generalized Gross–Pitaevskii equation, whereas the noncondensate (thermal) part is described by the quantum Boltzmann equation. However, the ZNG formalism cannot be directly applied to 1D systems or quasicondensates due to the fact that the fractional occupancy of the ground-state condensate mode in 1D does not dominate the occupancies of excited modes as it does in 3D, and hence a simple separation into a condensate and thermal excitations is not justified here.

## V. SUMMARY

In conclusion, we have studied the breathing oscillations of a harmonically trapped 1D Bose gas in the quasicondensate regime, invoked after a sudden quench of the trap frequency. Using the  $c$ -field approach for simulating the post-quench dynamics, we observed beating of two breathing modes oscillating with two distinct frequencies  $\omega_{Bi}$  ( $i=1, 2$ ), and each having their own damping rates  $\Gamma_i$ . The two breathing modes are attributed to low-energy particles in the bulk and high-energy particles in the tails of the density distribution of the gas. The bulk component breathes with the frequency close to the expected breathing mode frequency of a zero temperature system,  $\omega_{B1} \simeq \sqrt{3}\omega$ . On the other hand, the breathing mode frequency of the tail component is closer to that of a classical ideal gas,  $\omega_{B2} \simeq 2\omega$ . The damping rates  $\Gamma_1$  and  $\Gamma_2$ , extracted from the  $c$ -field simulations for typical experimental parameters, have the associated



damping time constants on the order of 0.25 s and 2.5 s, respectively.

We have also calculated the Landau damping rate  $\Gamma_L$  of the bulk component using the results of Ref. [54], and found that it is at last 3–4 times larger than the numerical value of  $\Gamma_1$  extracted from the  $c$ -field simulations. The discrepancy could be due to the breakdown of the assumption in the Landau theory of damping that the thermal excitations are in equilibrium. However, in the  $c$ -field simulations, the high-energy particles in the tails of the Bose gas are brought out of equilibrium after the quench and oscillate at their own collective frequency. As such, apart from causing the damping of the breathing oscillations in the bulk component due to the Landau mechanism, the tail component could also be driving the bulk at its own breathing frequency, thus extending the

lifetime of the respective oscillations and hence reducing the numerically observed damping rate  $\Gamma_1$ . Understanding this discrepancy warrants a further study, which could perhaps be accomplished by generalising the GNZ formalism to 1D systems, wherein the evolution of the entire  $c$ -field would be coupled to a quantum Boltzmann equation.

## ACKNOWLEDGMENTS

F. A. B. and K. V. K. acknowledge stimulating discussions with I. Bouchoule and M. J. Davis. K. V. K. acknowledges support by the Australian Research Council Discovery Project Grants DP170101423 and DP190101515.

- 
- [1] D. S. Jin, J. R. Ensher, M. R. Matthews, C. E. Wieman, and E. A. Cornell, Collective excitations of a Bose–Einstein condensate in a dilute gas, *Phys. Rev. Lett.* **77**, 420 (1996).
  - [2] D. S. Jin, M. R. Matthews, J. R. Ensher, C. E. Wieman, and E. A. Cornell, Temperature-Dependent Damping and Frequency Shifts in Collective Excitations of a Dilute Bose–Einstein Condensate, *Phys. Rev. Lett.* **78**, 764 (1997).
  - [3] D. M. Stamper-Kurn, H.-J. Miesner, S. Inouye, M. R. Andrews, and W. Ketterle, Collisionless and Hydrodynamic Excitations of a Bose–Einstein Condensate, *Phys. Rev. Lett.* **81**, 500 (1998).
  - [4] O. Maragò, G. Hechenblaikner, E. Hodby, and C. Foot, Temperature Dependence of Damping and Frequency Shifts of the Scissors Mode of a Trapped Bose–Einstein Condensate, *Phys. Rev. Lett.* **86**, 3938 (2001).
  - [5] F. Chevy, V. Bretin, P. Rosenbusch, K. W. Madison, and J. Dalibard, Transverse Breathing Mode of an Elongated Bose–Einstein Condensate, *Phys. Rev. Lett.* **88**, 250402 (2002).
  - [6] P. O. Fedichev, G. V. Shlyapnikov, and J. T. M. Walraven, Damping of Low-Energy Excitations of a Trapped Bose–Einstein Condensate at Finite Temperatures, *Phys. Rev. Lett.* **80**, 2269 (1998).
  - [7] L. Pitaevskii and S. Stringari, Landau damping in dilute Bose gases, *Physics Letters A* **235**, 398 (1997).
  - [8] L. Pitaevskii and S. Stringari, Elementary Excitations in Trapped Bose–Einstein Condensed Gases Beyond the Mean-Field Approximation, *Phys. Rev. Lett.* **81**, 4541 (1998).
  - [9] M. J. Bijlsma and H. T. C. Stoof, Collisionless modes of a trapped Bose gas, *Phys. Rev. A* **60**, 3973 (1999).
  - [10] U. Al Khawaja and H. T. C. Stoof, Kinetic theory of collective excitations and damping in Bose–Einstein condensed gases, *Phys. Rev. A* **62**, 053602 (2000).
  - [11] M. Guilleumas and L. P. Pitaevskii, Temperature-induced resonances and Landau damping of collective modes in Bose–Einstein condensed gases in spherical traps, *Phys. Rev. A* **61**, 013602 (1999).
  - [12] B. Jackson and C. S. Adams, Damping and revivals of collective oscillations in a finite-temperature model of trapped Bose–Einstein condensation, *Phys. Rev. A* **63**, 053606 (2001).
  - [13] B. Jackson and E. Zaremba, Quadrupole Collective Modes in Trapped Finite-Temperature Bose–Einstein Condensates, *Phys. Rev. Lett.* **88**, 180402 (2002).
  - [14] B. Jackson and E. Zaremba, Modeling Bose–Einstein condensed gases at finite temperatures with N-body simulations, *Phys. Rev. A* **66**, 033606 (2002).
  - [15] B. Jackson and E. Zaremba, Accidental Suppression of Landau Damping of the Transverse Breathing Mode in Elongated Bose–Einstein Condensates, *Phys. Rev. Lett.* **89**, 150402 (2002).
  - [16] B. Jackson and E. Zaremba, Landau damping in trapped Bose condensed gases, *New Journal of Physics* **5**, 88 (2003).
  - [17] M. Guilleumas and L. P. Pitaevskii, Landau damping of transverse quadrupole oscillations of an elongated Bose–Einstein condensate, *Phys. Rev. A* **67**, 053607 (2003).
  - [18] M. H. Anderson, J. R. Ensher, M. R. Matthews, C. E. Wieman, and E. A. Cornell, Observation of Bose–Einstein Condensation in a Dilute Atomic Vapor, **269**, 198 (1995).
  - [19] C. C. Bradley, C. A. Sackett, J. J. Tollett, and R. G. Hulet, Evidence of Bose–Einstein Condensation in an Atomic Gas with Attractive Interactions, *Phys. Rev. Lett.* **75**, 1687 (1995).
  - [20] K. B. Davis, M. O. Mewes, M. R. Andrews, N. J. van Druten, D. S. Durfee, D. M. Kurn, and W. Ketterle, Bose–Einstein Condensation in a Gas of Sodium Atoms, *Phys. Rev. Lett.* **75**, 3969 (1995).
  - [21] A. Griffin, T. Nikuni, and E. Zaremba, *Bose-Condensed Gases at Finite Temperatures* (Cambridge University Press, 2009).
  - [22] S. Beliaev, Energy spectrum of a non-ideal Bose gas, *Sov. Phys. JETP* **34**, 299 (1958).
  - [23] B. Fang, G. Carleo, A. Johnson, and I. Bouchoule, Quench-Induced Breathing Mode of One-Dimensional Bose Gases, *Phys. Rev. Lett.* **113**, 035301 (2014).
  - [24] T. Kinoshita, T. Wenger, and D. S. Weiss, A quantum Newton’s cradle, *Nature* **440**, 900 (2006).
  - [25] E. H. Lieb and W. Liniger, Exact Analysis of an Interacting Bose Gas. I. The General Solution and the Ground

- State, *Phys. Rev.* **130**, 1605 (1963).
- [26] E. H. Lieb, Exact Analysis of an Interacting Bose Gas. II. The Excitation Spectrum, *Phys. Rev.* **130**, 1616 (1963).
- [27] M. Rigol, V. Dunjko, and M. Olshanii, Thermalization and its mechanism for generic isolated quantum systems, *Nature* **452**, 854 EP (2008).
- [28] M. Rigol, Breakdown of Thermalization in Finite One-Dimensional Systems, *Phys. Rev. Lett.* **103**, 100403 (2009).
- [29] A. Polkovnikov, K. Sengupta, A. Silva, and M. Vengalattore, Colloquium: Nonequilibrium dynamics of closed interacting quantum systems, *Rev. Mod. Phys.* **83**, 863 (2011).
- [30] M. Kollar, F. A. Wolf, and M. Eckstein, Generalized Gibbs ensemble prediction of prethermalization plateaus and their relation to nonthermal steady states in integrable systems, *Phys. Rev. B* **84**, 054304 (2011).
- [31] J.-S. Caux and R. M. Konik, Constructing the generalized Gibbs ensemble after a quantum quench, *Phys. Rev. Lett.* **109**, 175301 (2012).
- [32] M. Gring, M. Kuhnert, T. Langen, T. Kitagawa, B. Rauer, M. Schreitl, I. Mazets, D. A. Smith, E. Demler, and J. Schmiedmayer, Relaxation and Prethermalization in an Isolated Quantum System, *Science* **337**, 1318 (2012).
- [33] T. Langen, S. Erne, R. Geiger, B. Rauer, T. Schweigler, M. Kuhnert, W. Rohringer, I. E. Mazets, T. Gasenzer, and J. Schmiedmayer, Experimental observation of a generalized Gibbs ensemble, *Science* **348**, 207 (2015).
- [34] I. E. Mazets, Integrability breakdown in longitudinally trapped, one-dimensional bosonic gases, *The European Physical Journal D* **65**, 43 (2011).
- [35] I. E. Mazets, T. Schumm, and J. Schmiedmayer, Breakdown of Integrability in a Quasi-1D Ultracold Bosonic Gas, *Phys. Rev. Lett.* **100**, 210403 (2008).
- [36] I. E. Mazets and J. Schmiedmayer, Thermalization in a quasi-one-dimensional ultracold bosonic gas, *New Journal of Physics* **12**, 055023 (2010).
- [37] S. Tan, M. Pustilnik, and L. I. Glazman, Relaxation of a High-Energy Quasiparticle in a One-Dimensional Bose Gas, *Phys. Rev. Lett.* **105**, 090404 (2010).
- [38] F. Möller, C. Li, I. Mazets, H.-P. Stimming, T. Zhou, Z. Zhu, X. Chen, and J. Schmiedmayer, Extension of the generalized hydrodynamics to the dimensional crossover regime, *Phys. Rev. Lett.* **126**, 090602 (2021).
- [39] T. Bland, N. G. Parker, N. P. Proukakis, and B. A. Malomed, Probing quasi-integrability of the gross-pitaevskii equation in a harmonic-oscillator potential, *Journal of Physics B: Atomic, Molecular and Optical Physics* **51**, 205303 (2018).
- [40] A. Bastianello, A. De Luca, B. Doyon, and J. De Nardis, Thermalization of a Trapped One-Dimensional Bose Gas via Diffusion, *Phys. Rev. Lett.* **125**, 240604 (2020).
- [41] K. F. Thomas, M. J. Davis, and K. V. Kheruntsyan, Thermalization of a quantum Newton's cradle in a one-dimensional quasicondensate, *Phys. Rev. A* **103**, 023315 (2021).
- [42] H. Moritz, T. Stöferle, M. Köhl, and T. Esslinger, Exciting Collective Oscillations in a Trapped 1D Gas, *Phys. Rev. Lett.* **91**, 250402 (2003).
- [43] E. Haller, M. Gustavsson, M. J. Mark, J. G. Danzl, R. Hart, G. Pupillo, and H.-C. Nägerl, Realization of an Excited, Strongly Correlated Quantum Gas Phase, *Science* **325**, 1224 (2009).
- [44] A. Sinatra, C. Lobo, and Y. Castin, Classical-field method for time dependent bose-einstein condensed gases, *Phys. Rev. Lett.* **87**, 210404 (2001).
- [45] C. Menotti and S. Stringari, Collective oscillations of a one-dimensional trapped Bose-Einstein gas, *Phys. Rev. A* **66**, 043610 (2002).
- [46] P. Pedri, D. Guéry-Odelin, and S. Stringari, Dynamics of a classical gas including dissipative and mean-field effects, *Phys. Rev. A* **68**, 043608 (2003).
- [47] R. Schmitz, S. Krönke, L. Cao, and P. Schmelcher, Quantum breathing dynamics of ultracold bosons in one-dimensional harmonic traps: Unraveling the pathway from few- to many-body systems, *Phys. Rev. A* **88**, 043601 (2013).
- [48] W. Tschischik, R. Moessner, and M. Haque, Breathing mode in the Bose-Hubbard chain with a harmonic trapping potential, *Phys. Rev. A* **88**, 063636 (2013).
- [49] A. I. Gudyma, G. E. Astrakharchik, and M. B. Zvonarev, Reentrant behavior of the breathing-mode-oscillation frequency in a one-dimensional Bose gas, *Phys. Rev. A* **92**, 021601 (2015).
- [50] S. Choi, V. Dunjko, Z. D. Zhang, and M. Olshanii, Monopole Excitations of a Harmonically Trapped One-Dimensional Bose Gas from the Ideal Gas to the Tonks-Girardeau Regime, *Phys. Rev. Lett.* **115**, 115302 (2015).
- [51] X.-L. Chen, Y. Li, and H. Hu, Collective modes of a harmonically trapped one-dimensional bose gas: The effects of finite particle number and nonzero temperature, *Phys. Rev. A* **91**, 063631 (2015).
- [52] I. Bouchoule, S. S. Szigeti, M. J. Davis, and K. V. Kheruntsyan, Finite-temperature hydrodynamics for one-dimensional Bose gases: Breathing-mode oscillations as a case study, *Phys. Rev. A* **94**, 051602 (2016).
- [53] C. J. E. Straatsma, V. E. Colussi, M. J. Davis, D. S. Lobsenz, M. J. Holland, D. Z. Anderson, H. J. Lewandowski, and E. A. Cornell, Collapse and revival of the monopole mode of a degenerate Bose gas in an isotropic harmonic trap, *Phys. Rev. A* **94**, 043640 (2016).
- [54] Z.-J. Yang, Z.-L. Chai, C.-X. Li, and X.-D. Ma, Landau Damping of Collective Mode in a Quasi-One-Dimensional Repulsive Bose-Einstein Condensate, *Communications in Theoretical Physics* **57**, 789 (2012).
- [55] F. Bayocboc Jr, M. Davis, and K. Kheruntsyan, Dynamics of thermalization of two tunnel-coupled one-dimensional quasicondensates, arXiv preprint arXiv:2108.13095 (2021).
- [56] Y. Castin, R. Dum, E. Mandonnet, A. Minguzzi, and I. Carusotto, Coherence properties of a continuous atom laser, *Journal of Modern Optics* **47**, 2671 (2000).
- [57] P. Blakie, A. Bradley, M. Davis, R. Ballagh, and C. Gardiner, Dynamics and statistical mechanics of ultra-cold Bose gases using c-field techniques, *Adv. Phys.* **57**, 363 (2008).
- [58] In the present work, the high-energy cutoff  $\epsilon_{cut}$  was effectively imposed by the choice of the numerical grid for simulations (carried out in the harmonic oscillator, Hermite-Gaus basis) rather than through the explicit projection operator. This is because the classical field predictions in 1D (unlike in 3D) depend on  $\epsilon_{cut}$  only very weakly once  $\epsilon_{cut}$  is chosen sufficiently large [41, 52, 55, 67–70]. All simulations were performed using the software package XMDS2 [71].
- [59] K. V. Kheruntsyan, D. M. Gangardt, P. D. Drummond, and G. V. Shlyapnikov, Finite-temperature correlations

- and density profiles of an inhomogeneous interacting one-dimensional Bose gas, [Phys. Rev. A \*\*71\*\*, 053615 \(2005\)](#).
- [60] O. Penrose and L. Onsager, Bose–Einstein Condensation and Liquid Helium, [Phys. Rev. \*\*104\*\*, 576 \(1956\)](#).
  - [61] C. Mora and Y. Castin, Extension of Bogoliubov theory to quasicondensates, [Phys. Rev. A \*\*67\*\*, 053615 \(2003\)](#).
  - [62] M. A. Cazalilla, Bosonizing one-dimensional cold atomic gases, [J. Phys. B \*\*37\*\*, S1 \(2004\)](#).
  - [63] I. Bouchoule, M. Arzamasovs, K. V. Kheruntsyan, and D. M. Gangardt, Two-body momentum correlations in a weakly interacting one-dimensional Bose gas, [Phys. Rev. A \*\*86\*\*, 033626 \(2012\)](#).
  - [64] P. Deuar, A. G. Sykes, D. M. Gangardt, M. J. Davis, P. D. Drummond, and K. V. Kheruntsyan, Nonlocal pair correlations in the one-dimensional Bose gas at finite temperature, [Phys. Rev. A \*\*79\*\*, 043619 \(2009\)](#).
  - [65] D. S. Petrov, G. V. Shlyapnikov, and J. T. M. Walraven, Regimes of Quantum Degeneracy in Trapped 1D Gases, [Phys. Rev. Lett. \*\*85\*\*, 3745 \(2000\)](#).
  - [66] E. Zaremba, T. Nikuni, and A. Griffin, Dynamics of Trapped Bose Gases at Finite Temperatures, [Journal of Low Temperature Physics \*\*116\*\*, 277 \(1999\)](#).
  - [67] J. Pietraszewicz and P. Deuar, Classical field records of a quantum system: Their internal consistency and accuracy, [Phys. Rev. A \*\*92\*\*, 063620 \(2015\)](#).
  - [68] J. Pietraszewicz and P. Deuar, Complex wave fields in the interacting one-dimensional bose gas, [Phys. Rev. A \*\*97\*\*, 053607 \(2018\)](#).
  - [69] J. Pietraszewicz and P. Deuar, Classical fields in the one-dimensional bose gas: Applicability and determination of the optimal cutoff, [Phys. Rev. A \*\*98\*\*, 023622 \(2018\)](#).
  - [70] S. A. Simmons, F. A. Bayocboc, J. C. Pillay, D. Collas, I. P. McCulloch, and K. V. Kheruntsyan, What is a Quantum Shock Wave?, [Phys. Rev. Lett. \*\*125\*\*, 180401 \(2020\)](#).
  - [71] G. R. Dennis, J. J. Hope, and M. T. Johnsson, Xmds2: Fast, scalable simulation of coupled stochastic partial differential equations, [Computer Physics Communications \*\*184\*\*, 201 \(2013\)](#).